

# Parametrization of Multiple Pathways in Proteins: Fast Folding versus Tight Transitions

Paul G. Dommersnes,\* Alex Hansen,\* Mogens H. Jensen, and Kim Sneppen  
*Niels Bohr Institute and NORDITA, Blegdamsvej 17, DK-2100 Copenhagen Ø, Denmark*  
(February 1, 2008)

Growing experimental evidence shows that proteins follow one or a few distinct paths when folding. We propose in this paper a procedure to parametrize these observed pathways, and from this parametrization construct effective Hamiltonians for the proteins. We furthermore study the denaturated-native transitions for a wide class of possible effective Hamiltonians based on this scheme, and find that the sharpness (tightness) of the transitions typically are close to their theoretical maximum and thus in quantitative accordance with the sharp folding transition observed for single domain proteins. Finally we demonstrate that realistic folding times are typical for the proposed class of Hamiltonians, and we discuss the implication of the predicted entropy barriers on the temperature dependence of the folding times.

PACS: 05.70.Jk, 82.20.Db, 87.15.By, 87.10.+e

## I. INTRODUCTION

Globular proteins exists in two states the native, or folded, state and the denaturated, or unfolded, state [1]. The folding of a protein is mostly driven by thermodynamics, and it typically occurs on a time scale of order seconds. The folding, and the resulting conformations result from an interplay between polar and nonpolar amino acids on the protein, their hydrogen bonds, and how all these interact with and constrain the surrounding water. The folding is therefore an immensely complex process and to date it is still a completely open problem how one may predict a protein's folding properties given its structure.

On a qualitative level it is remarkable that the native state of a globular protein is solid with specified positions of all amino acids. This fact is thermodynamically reflected in a denaturation phase transition which is exceedingly sharp, in spite of the small number of molecules in the protein. Enhancing this qualitatively remarkable phenomenon is the fact that a typical polymer folds with a very weak transition [2]. In fact single domain protein folding transition fairly accurately behaves as a two-state thermodynamical system [3] where only denatured and native state can be populated and nearly no states with energies between these two extremal states are observed. Another remarkable feature of proteins is that they reach their unique ground state in a time that is much smaller than the time needed to search the extremely large configurational space. This is commonly known as the Levinthal paradox, and is noteworthy because it is difficult to merge with the two-state thermodynamics of proteins.

Research into the more specific aspects of the dynamics of protein folding is divided into several sub camps. For example, there is a huge effort to study simplified models numerically using ideas originating from spin glass theory. The basic idea here is that the different possible conformations of a protein define an energy landscape containing multiple minima. Such a picture is supported by experimental evidence at very low temperatures and structures confined by potentials less than about 2kcal/mol [4]. However, if the dynamics of proteins at normal temperatures were that of spin glasses, its folding would be even slower than a random search in configuration space, resulting in time scales on an astronomical scale. This is not the case. Today, one imagines two possible ways to explain how proteins can fold on reasonable timescales: (1) The existence of *folding funnels* [5–7], or (2) the existence of *folding pathways* [8,9]. The basic idea behind the folding funnel is that it is a deformation of the energy landscape in such a way that it resembles a funnel. The protein then “falls” into the global ground state without getting stuck.

The folding pathway is a concept related to a specific sequence of events. In contrast to a funnel, a pathway is characterized by subsequent formation of identifiable structures that must be formed in a specific order. Pathway studies of proteins that fold have been extensively carried out by Fersht [10]. Occasionally one observes more than one possible pathway. The mechanism leading to the existence of guiding pathways may be hierarchical from small scales to larger scales in the sense of Baldwin and Rose [8,9], or it may be purely sequential as suggested in [11]. It

---

\*Permanent address: Department of Physics, Norwegian University of Science and Technology, NTNU, N-7491 Trondheim, Norway

is the aim of this paper to demonstrate a third possibility, that encompass both of the above suggested scenarios but do it in a way that ensure the experimentally observed two state nature of protein folding-unfolding.

In the next section, we introduce and discuss our parametrization scheme for protein folding. This is based on our earlier work on one-pathway protein folding [11–13]. In order for a protein to be biologically relevant, certain demands has to be put on its folding properties. One such demand is that the folding-unfolding transition is sharp. The sharpest possible transition is obtained when the system is two state. We analyse in Section III a class of Hamiltonians parametrized by the scheme outlined in Section II B with respect to sharpness using the van’t Hoff relation. We find that the *typical* system within this class behaves as a two-state system with maximal sharpness of transition. In Section IV, we finally demonstrate that the class of Hierarchical folders encoded by the parametrization scheme of Section II have folding times compatible with the ones that are experimentally observed. Further we demonstrate that the phase transition is sharpened by an entropic barrier and therefore that the folding time increase strongly with temperature  $T$  in some  $T$  interval below the equilibrium transition temperature  $T_c$ . In Section V we conclude that both demands, the sharpness of transition and the short folding times, are encoded by sequentially encoded hierarchical folders.

## II. PATHWAYS

We take the point of view that proteins follow certain pathways when folding from the denaturated to the native state. The “standard” theorist’s way of envisionin such a pathway is as a curve in some rugged energy landscape leading to the global minimum point — which corresponds to the native state. In the present work, we take a different point of view. We define a pathway as a *sequence of partially folded structures* which sequentially reduces both energy and entropy of the protein, and thus guide it towards the native state. By a partially folded structure we mean a protein conformation where parts of it has taken on the structure of the native state.

The simplest model of subsequent entropy pruning is a zipper [14], where one at each step  $k$  of the folding gains one unit of energy, say  $E(n+1) = E(n) - a$ , and simultaneously reduces the available number of conformational states with a factor  $g$ , i.e., state space  $S(k) \rightarrow S(k+1) = S(k)/g$ . If each step is associated with binding of one amino acid from a random coil then  $g \sim 6$  corresponding to the possible orientations of one amino acid along the chain [1]. If we deal with reduction of effective number of orientations form a compact molten globule, then  $g \sim 6/e \sim 2$  where the factor  $e$  comes from excluded volume effects [15]. For individual amino acid contacts the corresponding energy gains may be estimated from the Miyazawa-Jernigan matrix [16], suggesting energies  $a$  of order  $1 \rightarrow 2$  kcal/mol. In the first subsection we will explore the mathematical formulation of this simple zipper model, and demonstrate that it indeed predicts a first order phase transition, albeit a fairly weak one.

Folding of real proteins are presumably more complicated than a simple zipper. Protein structure data collected by Baldwin and Rose [8,9] support that the native state of real proteins is reached from progressively larger parts of the protein which are stabilized by the smaller structures already in place. This indeed suggest a sequential ordering of events with some similarity to the zipper, but with the important difference that folding may initiate at different places along the amino acid chain simultaneously. If this was the case, the resulting independence of events would imply a factorization of the partition function into sub-parts, with the result of weakening or eventually destroying the phase transition altogether. As discussed in Section III, the melting phase transition of a single domain protein is remarkably sharp, implying that folding the protein is a very cooperative and correlated process.

We will in Section III see that the observed sharpness of the phase transition of proteins puts severe constraint on any protein folding model, e.g. ruling out both the simplest version of the zipper model and the simplest version of the hierarchy model. In addition, there is growing evidence that proteins may follow alternate pathways during the folding process [3,9,17–19], thus requiring a formalism that merge the conflicting interest between the need of dealing with more than one pathway, to fold in a reasonable time, and to maintain the native state sharply folded when it finally is reached.

The purpose of this section is to develop such a formalism, thus encompassing both the pathway formalism and the possibility that folding proceed hierarchically from smaller to larger structures. We first assume that there is only one pathway. This will allow us to introduce the central ideas in our approach in the next subsection. In subsection II B we subsequently generalize theses ideas into a scenario where several pathways are allowed.

## A. Single Pathway

A folding pathway is a sequence of partially folded structures. Each structure along the pathway may contain the previously folded structures as a subset. If there is only one pathway available for the protein, this will be the case. We are therefore dealing with a hierarchy where structures use previously folded structures as building blocks. It is also clear that the folding process towards the native state proceeds from smaller to larger scales.

We number the partially folded structures as they appear in the folding process,  $i = 1, \dots, N$ . The binary variable  $\psi_i$  equals 1 if partially folded structure  $i$  exists — also if it forms part of an even larger folded structure. Otherwise, it is zero. Thus, the folding pathway may be parametrized by the sequence of inequalities

$$\psi_1 \geq \psi_2 \geq \psi_3 \geq \dots \geq \psi_N . \quad (1)$$

We will in the following refer to the  $\psi_i$  variables as *folding variables*.

There is energy and entropy associated with the partially folded structures. There are the direct binding energies that keeps the folded structures together. Perturbing the folded parts of the protein requires more energy than perturbing the unfolded parts. The latter may change conformation with very low or no energy cost. Thus, these changes appear as entropy on the thermodynamical level. In order to model these mechanisms, we introduce a second set of variables, the *structural variables*  $\xi_1$  to  $\xi_N$ . These variables contain e.g. the angles  $\phi$  and  $\psi$  associated with  $N - C_\alpha$  and the  $C_\alpha - C'$  bonds of the part of the protein that folded. However, they are simplifications — and to simplify even further, we assume that they only take two values [13],

$$\xi_i = \begin{cases} 1 , \\ 1 - \Xi . \end{cases} \quad (2)$$

This latter simplification is not essential to retain an analytically tractable model. However, it makes it easier to introduce the model and discuss it in general terms. The choice of two states corresponds to a degeneracy factor  $g = 2$ , and one can easily generalize the results we will obtain to larger  $g$  values by simply assuming that  $g - 1$  states are associated with the higher energy level.

We now proceed to construct the simplest possible Hamiltonian that reflect the above discussion [13]. It is

$$\mathcal{H} = - \sum_{i=1}^N a^{(i)} \psi_i \xi_i , \quad (3)$$

where  $a^{(i)}$  are positive coupling constants.

When the protein is at stage  $j$  in the folding process, the energy associated with it is

$$E_j = \sum_{i=1}^j \xi_i . \quad (4)$$

The parts of the protein not yet folded provide entropy, which in this particular case consists of the variables  $\xi_{j+1}, \dots, \xi_N$ . The degeneracy of this protein configuration is  $2^{N-j}$ .

Working with the Hamiltonian Eq. (3) with the constraints (1) is somewhat cumbersome. We will therefore make a coordinate transformation that builds the constraints into the Hamiltonian directly. As we will see in the next section, this transformation allows us to generalize the one-pathway Hamiltonian presented in this section to multiple-pathway Hamiltonians: Specify a set of pathways, and the corresponding Hamiltonian can be written down immediately.

We assume in the following that the value  $\Xi$  defined in Eq. (2) is so large that the  $\xi_i$ 's for which  $\psi_i = 1$ , will not take on this value for any realistic temperature ( $T < 100$  C). In this case, we may set

$$\begin{aligned} \psi_1 &= \phi_1 , \\ &\vdots \\ \psi_i &= \phi_1 \phi_2 \cdots \phi_i , \\ &\vdots \\ \psi_N &= \phi_1 \phi_2 \cdots \phi_i \cdots \phi_N , \end{aligned} \quad (5)$$

where there are no constraints on the new variables  $\phi_i$ . We see that the constraints Eq. (1) automatically are obeyed. The Hamiltonian (3) now becomes

$$\mathcal{H} = -a^{(1)}\phi_1 - a^{(2)}\phi_1\phi_2 - \dots - a^{(N)}\phi_1 \dots \phi_N, \quad (6)$$

We furthermore note that the degeneracy provided by the  $\xi_i$  variables (as they may take on two possible values, 1 and  $1 - \Xi$ , when the corresponding  $\psi_i$  is zero), is also build into the Hamiltonian. Assume e.g. that all  $\phi_1$  to  $\phi_j$  are equal to one, this corresponds to  $\psi_1 = \dots \psi_j = 1$ . Furthermore assume that  $\phi_{j+1} = \psi_{j+1} = 0$ . The remaining  $\phi_{j+2}$  to  $\phi_N$  can take on any value without change in energy. Thus, to within a factor 2, the degeneracy is the same that provided by the  $\xi_i$  variables in the original Hamiltonian (3).

The Hamiltonian (6) has a first order transition at a temperature  $T = 1/\log 2$  when  $a^{(1)} = \dots = a^{(N)} = 1$  [11]. This Hamiltonian is easily generalized to take into account the coupling between water and protein [13].

## B. Multiple Pathways

We need to define what we mean by “multiple pathways.” We return to the single pathway defined using the folding variables by Eq. (II A). Suppose we break this sequence of inequalities by removing one of them, say  $\psi_i \geq \psi_{i+1}$ , so that we have

$$\psi_1 \geq \dots \geq \psi_i, \quad (7)$$

and

$$\psi_{i+1} \geq \dots \geq \psi_N. \quad (8)$$

Now, the status (0 or 1) of any  $\psi_j$ , where  $j \leq i$  is independent of the status of any  $\psi_k$ , where  $k > i$ . That is, we have created two independent folding “domains.”

In terms of the  $\phi_i$  variables, the two groups of inequalities (7) and (8), may be expressed as

$$\begin{aligned} \psi_1 &= \phi_1, \\ &\vdots \\ \psi_i &= \phi_1 \dots \phi_i, \end{aligned} \quad (9)$$

and

$$\begin{aligned} \psi_{i+1} &= \phi_{i+1}, \\ &\vdots \\ \psi_N &= \phi_{i+1} \dots \phi_N. \end{aligned} \quad (10)$$

We may also construct the corresponding Hamiltonian,

$$\mathcal{H} = -a^{(1)}\phi_1 - a^{(2)}\phi_1\phi_2 - \dots - a^{(i)}\phi_1 \dots \phi_i - a^{(i+1)}\phi_{i+1} - \dots - a^{(N)}\phi_{i+1} \dots \phi_N. \quad (11)$$

When setting up the Hamiltonian (11), we have made the assumption that both pathways,  $1 \rightarrow 2 \rightarrow \dots \rightarrow i$  and  $(i+1) \rightarrow \dots \rightarrow N$  have the same degeneracies associated with them, fixing the relative entropic contribution from each branch. By introducing additional independent variables  $\phi_{N+j}$ , we may tailor these contributions. For example, the Hamiltonian

$$\mathcal{H} = -a^{(1)}\phi_1 - a^{(2)}\phi_1\phi_2 - \dots - a^{(i)}\phi_1 \dots \phi_i - a^{(i+1)}\phi_{i+1}\phi_{N+1} - \dots - a^{(N)}\phi_{i+1} \dots \phi_N\phi_{N+1} \quad (12)$$

will increase the entropic contribution of the second branch by  $T \log 2$  compared to the first branch.

We may generalize the ideas presented above to systems with multiple folding pathways. This is done simply by generating telescoping groups of  $\phi_i$  variables, one for each pathway. The corresponding Hamiltonian may be written down directly,

$$\mathcal{H} = - \sum_i a_i^{(1)} \phi_i - \sum_{i \neq j} a_{ij}^{(2)} \phi_i \phi_j - \dots - \sum_{i \neq j \neq k \dots} a_{ijk\dots}^{(N)} \phi_i \phi_j \phi_k \dots \quad (13)$$

We have here added subscripts to the  $a^{(i)}$  coefficients, reflecting which  $\phi_i$  variables are involved in the corresponding term in the Hamiltonian.

In order to construct a Hamiltonian given a set of pathways, we start with organizing the pathways in a branching structure where each numbering refer to a folded substructure of the protein, as shown in Fig. 1. The interpretation of this figure is that folding of structures 1 and 5 are independent starting points of the folding process. In order to structure 4 to be formed, structure 5 must already be in place. However, this structure is independent of structure 1 having been formed. Structure 2, on the other hand, needs both structures 1 and 5 in place. Lastly, structure 3 can only form if both structures 2 and 4 have formed. In the end, all structures must always be formed. A concrete example of such a set of pathways has been reported for staphylococcal nuclease [20,21].

Assuming now that the reduction in degeneracy when either structure 1 or 5 form is the same, we may set up a “folding table” as shown in Table I. From this table, we read off the Hamiltonian

$$\mathcal{H} = -a_1^{(1)} \phi_1 - a_5^{(1)} \phi_5 - a_{45}^{(2)} \phi_4 \phi_5 - a_{125}^{(3)} \phi_1 \phi_2 \phi_5 - a_{12345}^{(5)} \phi_1 \phi_2 \phi_3 \phi_4 \phi_5 . \quad (14)$$

In the following, we will study the thermodynamical and dynamical properties of Hamiltonians constructed in this way. There are two main questions to be addressed which are essential in connection with protein folding: (1) sharpness of folding transition and (2) shortness of folding time. In the next section, we will consider the sharpness of the transition.

### III. SHARPNESS OF TRANSITION

An excellent measure of sharpness of a first-order transition is to study the van’t Hoff relation [22,23] which relates enthalpy change through the transition  $\Delta H$ , the peak of the heat capacity  $C_p$ , the absorbed heat,  $Q$  through the formula

$$\Delta H = \alpha \frac{T_c^2 C_p(T_c)}{Q} . \quad (15)$$

Here  $T_c$  is the transition temperature, and  $\alpha$  is the *van’t Hoff coefficient*. The smaller this coefficient is, the sharper the transition.

We may demonstrate this in the following way. In the present case,  $\Delta H = Q$  (as there is no pressure in the system), which is the area of the bump in the heat capacity plot. The height of the hump,  $h$ , is  $C_p$ , while the area  $Q$  is essentially the width of the top  $b$  multiplied by the height,  $h$ ,  $Q = bh$ . We may thus write the van’t Hoff equation

$$b^2 h = \alpha T_c^2 . \quad (16)$$

From this equation it might seem that the opposite of what we are claiming is true: The larger the  $\alpha$ , the wider the transition, as the height  $h$  is proportional to  $\alpha$ . However, one must not forget the presence of the width  $b$ . We rewrite the left hand side of Eq. (16) as

$$(bh)^2 \frac{1}{h} = \alpha T_c^2 . \quad (17)$$

Now keeping the area of the hump,  $bh = Q$ , constant, we see that the height  $h$  is *inversely* proportional to  $\alpha$ . Hence, our statement that a smaller  $\alpha$  implies a sharper transition follows, as sharpness is a relative concept.

In order to understand the the  $\alpha$  coefficient properly, we examine its physical meaning in the following. Let us assume a system with an equally spaced energy spectrum,  $1, \dots, N$ . We furthermore assume a degeneracy  $g_n$  for the  $n$ th energy level. The partition function is then

$$Z = \sum_{n=0}^N g_n e^{n/T} . \quad (18)$$

For proteins there should be a unique ground state, so that  $g_N = 1$ . The energy is given by

$$E(T) = T^2 \frac{\partial}{\partial T} \log Z = -\langle n \rangle, \quad (19)$$

and the heat capacity is given by

$$C(T) = \frac{\partial}{\partial T} E(T) = \frac{\langle n^2 \rangle - \langle n \rangle^2}{T^2}. \quad (20)$$

These relations are of course valid at any temperature. The  $\alpha$  factor can now be expressed in terms of the fluctuations of the energy levels at  $T = T_c$ ,

$$\langle n^2 \rangle - \langle n \rangle^2 = \frac{N^2}{\alpha}. \quad (21)$$

For *any* probability distribution we must have  $\langle n^2 \rangle - \langle n \rangle^2 \leq N^2/4$ . We only have equality when  $P(n=0) = P(n=N) = 1/2$ . Thus in general

$$\alpha \geq 4. \quad (22)$$

Equality  $\alpha = 4$  is only found when the system exhibits two state behaviour, i.e., when  $g_0 = g_N e^{N/T}$  and otherwise  $g_n = 0$ . This is fulfilled with the Hamiltonian  $\mathcal{H} = -N\phi_1 \cdots \phi_N$ , i.e., when all terms  $a^{(i)} = 0$  for all  $i < N$  in Eq. (11). In general Eq. (21) can be reformulated as

$$\langle s^2 \rangle - \langle s \rangle^2 = \frac{1}{\alpha}. \quad (23)$$

which express  $\alpha$  as the variance of the distribution of normalized energy states ( $s = n/N$ ) at the transition point. This distribution could be bimodal, ( $\alpha = 4$ ), be flat ( $\alpha = 12$ ) or be centered around a mean intermediate energy ( $\alpha > 12$ ). The flat distribution is obtained when all  $a^{(i)} = \text{const}$  in the Hamiltonian (11). Of special interest is the class of Hamiltonians that correspond to the hierarchical folding suggested by Baldwin and Rose [8,9]. We show in Fig. 2 an example of such a hierarchical folding network with four levels. In this scheme the folding of smaller units form a necessary but not sufficient condition for the folding of larger units. A corresponding Hamiltonian may be constructed as outlined in Section IIB, and we find

$$\mathcal{H} = -a_1^{(1)}\phi_1 - a_2^{(1)}\phi_2 - a_3^{(1)}\phi_3 - a_4^{(1)}\phi_4 - a_{125}^{(3)}\phi_1\phi_2\phi_5 - a_{346}^{(3)}\phi_3\phi_4\phi_6 - a_{1234567}^{(7)}\phi_1\phi_2\phi_3\phi_4\phi_5\phi_6\phi_7. \quad (24)$$

At each level in the hierarchy a new variable is needed in order to make folding at level below a necessary but sufficient condition for folding at this level.

As the number of terms in this hierarchical Hamiltonian grows,  $\alpha \rightarrow \infty$ . The reason for this is the statistical broadening due to the exponentially growing number of independent branches when moving “backwards” in the hierarchy towards smaller units.

Privalov and Khechinavili [22] measured experimentally the value

$$\alpha = 4.2 \pm 0.2. \quad (25)$$

for large group of small globular proteins. Thus real single domain proteins are close to two-state behaviour, i.e., far from a simply guided Hamiltonian, and very far from protein folding viewed as subsequent folding of independent subunits. Folding of single domain proteins, that in practical terms means proteins of about 100 amino acids is indeed close to a maximally cooperative process.

#### A. A Class of Hierarchical Hamiltonians with $\alpha = 4$ .

Based on spatial correlations of amino acids in real proteins, Baldwin and Rose argue convincingly that some sort of subsequent folding hierarchy must be implemented in real protein folding [8,9]. In last section we saw that the simplest hierarchical scheme is excluded for single domain proteins. We now explore a more elaborate hierarchical scheme, where correlations between folding subunits naturally becomes implemented on an early level. The simplest of these is the single pathway model of Eq. (6). A general formulation is the Hamiltonian (13). It has up to  $N$  groups of products of various length of  $\phi_i$  variables. We will in next subsection investigate the broad subclass of these Hamiltonians which are restricted by having maximum one term of each product number, and see that they typically

have  $\alpha \approx 4$ . This means that we investigate Hamiltonians as in Eq. (13) where the coefficient  $a_{ijk\dots}^{(n)} = 1$  for one combination of  $ijk\dots$  and otherwise zero. Thus, there is one term with only one  $\phi_i$ , one term with two  $\phi_i$  variables etc.

We note that the folding system in Fig. 1 as described by Eq. (14) does not include only one term at each level. However, the system in Fig. 1 can also be parametrized by introducing one additional auxiliary variable  $\phi_6$ , thereby creating an entropy barrier in the thermodynamics. The corresponding Hamiltonian for Fig. 1 would then be

$$\mathcal{H} = -a_1^{(1)}\phi_1 - a_5^{(1)}\phi_5\phi_6 - a_{456}^{(3)}\phi_4\phi_5\phi_6 - a_{1256}^{(4)}\phi_1\phi_2\phi_5\phi_6 - a_{123456}^{(6)}\phi_1\phi_2\phi_3\phi_4\phi_5\phi_6. \quad (26)$$

This is the type of Hamiltonians that we wish to study. This subclass deals with systems where indeed different regions may start independent folding, but where some foldings are more difficult to initiate and thus becomes rate limiting. In other words, that different events takes very different times implies that some folding events acts as effective nucleation centers. When these barriers are overcome, subsequent foldings spread across the system along some fairly well defined paths.

The nucleation barriers were associated to cases where several variables must fold simultaneously without previous guiding ( $\phi_5$  and  $\phi_6$  in the above Hamiltonian (26)). In addition, different folding paths typically become correlated e.g. through a common origin, as in the above Hamiltonian where the events  $\phi_5$  and  $\phi_6$  both are needed in order to proceed folding along the parallel ways parametrized by respectively  $\phi_2$  and  $\phi_4$ . Such correlation could e.g. be due to steric interactions that facilitate folding by bringing far-apart amino acids closer to each other. These associated entropy barriers and correlations are responsible for the effective two state behaviour that this class of hierarchical models exhibit. We will examine this in detail in the next section.

## B. Averaging over the Class of Hamiltonians

We will in following show that the type of Hamiltonians discussed in the previous section displays remarkable thermodynamic properties. We shall consider more specifically the class of Hamiltonians defined by Eq. (13), where there is only one term for each number of  $\phi_i$ s. The partition function for a Hamiltonians belonging to this class is

$$Z = \sum_{\{\phi\}} e^{-\mathcal{H}/T}. \quad (27)$$

To gain insight into the thermodynamics of this class of Hamiltonians, we have calculated the mean of the partition function over all possible Hamiltonians. The result is

$$\langle Z \rangle = 1 + \sum_{s=1}^N \binom{N}{s} \prod_{k=1}^s \left[ 1 + \frac{s!(N-k)!}{N!(s-k)!} (e^{1/T} - 1) \right]. \quad (28)$$

The calculation is outlined in Appendix A. This gives us the thermodynamics of an average Hamiltonian. In order to find out if this is a representative result we have to calculate the fluctuations around this mean. All thermodynamics properties of a given Hamiltonian is derived from  $\log Z$ , and the mean can be expressed as  $\langle \log Z \rangle = \langle \log z \rangle + \log \langle Z \rangle$ , with  $z = Z/\langle Z \rangle$ . We have in Appendix B transformed the expression for the fluctuations of the partition function into the function, Eq. (B6) and the result is plotted in Fig. 3. The fluctuations are extremely small, in fact  $\langle z^2 \rangle - \langle z \rangle^2 \rightarrow 0$  as the system size increases. For example for  $N \sim 100$  they contribute  $\sim 10^{-4} k_B T$  to the free energy, and hence without any physical relevance. In other words two randomly chosen Hamiltonians will have exactly the same thermodynamic properties, the system is *self-averaging* and Eq. (28) is the exact solution of the partition function.

In order to study the folding transition, we define an order parameter,  $u$ , by the mean of the sum over all the  $\phi$  variables

$$u = \frac{2}{N} \sum_{i=1}^N \langle \phi_i \rangle - 1. \quad (29)$$

When the protein is in the ground state  $\langle \phi_i \rangle = 1$  and the order parameter is  $u = 1$ , at high temperatures  $\langle \phi_i \rangle = 1/2$  and  $u = 0$ . Since the class of hamiltonians that we study are self-averaging for large  $N$ , we may calculate the thermal mean values by taking the average over all Hamiltonians. We may thus write

$$\begin{aligned}
\sum_i \langle \phi_i \rangle &= \frac{1}{M} \sum_{\{a\}} \sum_{\{\phi\}} \sum_i \phi_i e^{-\mathcal{H}/T} / \langle Z \rangle \\
&= \frac{1}{\langle Z \rangle} \sum_{s=1}^N s \binom{N}{s} \prod_{k=1}^s \left[ 1 + \frac{s!(N-k)!}{N!(s-k)!} (e^{1/T} - 1) \right],
\end{aligned} \tag{30}$$

where  $M$  is the total number of Hamiltonians. Fig. 4 shows the order parameter at different temperatures. We clearly see that there is sharp first-order transition around the temperature  $T_c \sim 1.44$ . The sharpness of the transition is characterized by the van't Hoff  $\alpha$  coefficient, which is calculated from the partition function Eq. (28). The results plotted in Fig. 5 show that it goes quickly to  $\alpha = 4$  for large  $N$ , which is the lowest possible value, i.e. the sharpest possible transition. We conclude hence that the folding scheme we have introduced gives a first-order phase transition with a van't Hoff coefficient of  $\alpha \sim 4$ , corresponding to a *two-state* thermodynamics.

We note that for the single-path Hamiltonian, Eq. (6) with all  $a^{(i)} = 1$ ,  $\alpha$  equals 12. However, if the last term is set equal to  $a^{(N)} = \epsilon N$ , where  $\epsilon \rightarrow 0$  is small (and goes to zero as  $N$  in the limit  $N \rightarrow \infty$ ), then  $\alpha \approx 4$  [24].

#### IV. FOLDING TIME

Proteins in their native form have well defined structures that are separated from their denatured counterparts through some barrier, as quantified by value of  $\alpha$ . The denatured state consists of an astronomical numbers of microscopic conformations, whereas the native state is unique. The fact that the unique native state anyway is reached fairly fast from this large number of unfolded configurations is known as the Levinthal paradox. Thus, the folding proteins must have some property encoded which lower configurational entropy systematically as folding proceeds. However, such guided folding has to be merged with the fact that the folding process exhibits effectively two-state behaviour, i.e. has few or no detectable intermediates [25], respectively  $\alpha \sim 4$  [23].

Minimalization of folding time and the van't Hoff parameter  $\alpha$  poses seemingly contradictory goals. This one might expect because absence of significant intermediates restricts the possibility of guided folding between the denatured states and the native state. As an example the following Hamiltonian has  $\alpha = 4$ , i.e., a maximally sharp transition [24],

$$\mathcal{H} = -N \phi_1 \phi_2 \cdots \phi_N. \tag{31}$$

However, it has absolutely no guiding at all: When in the denatured state, i.e., when at least one  $\phi_i = 0$ , there is no energy gain in turning this to  $\phi_i = 1$ , unless all other variables  $\phi_j$  already are equal to one. There is no energy gain unless such a protein moves into the native state. Searching for the native state in this system will grow exponentially with system size  $N$ . In general, it may seem that the more “two state” the transition is, the less guiding can be involved, and hence, the longer the folding time will be.

In order to discuss folding times, we need an operational definition of folding time. We base our definition on the one-step Monte Carlo method [26]. The Monte Carlo method is a way to generate a biased random walk through configuration space such that the relative frequency of occupancy of any configuration is proportional to the Boltzmann factor. Thus Monte Carlo “time”, measuring the number of steps of the random walk, has strictly speaking nothing to do with “real” time. However, in a discrete system, such as our model, we believe that time defined in this way, essentially brings us as close as possible to time in a corresponding continuous system. Hence, we will base our definition of time in the model by one-step Monte Carlo. Hence, we define one unit of time as the times where all variables have been updated once in average. This definition of time is common when dealing with dynamical questions concerning discrete system [26].

The non-guided Hamiltonian (31) will fold in a time proportional to  $2^N/N$  when starting from a random initial configuration. The fully guided (zipper) Hamiltonian (6) will similarly fold in a time proportional to  $N$ . The Baldwin-Rose picture of hierarchical folding [8,9] will give a folding time proportional to  $\log N$ . These examples, as noted above, seem to suggest that Hamiltonians with larger  $\alpha$  fold faster. However real single-domain proteins have  $\alpha$  close to its minimum value 4, and are still able to fold in fairly short time.

We have in Section III A suggested a class of hierarchical folders, and seen that these typically have  $\alpha \sim 4$  that is compatible with two-state behaviour seen in experiments.

In order to examine the folding behavior, we restrict ourselves initially to the case of zero temperature, i.e., when a term has folded it never opens again. The fact that we at all can reach the ground state at zero temperature follows from all terms in the Hamiltonian being attractive (i.e., negative signs) and that the various terms in the Hamiltonian



guide the system toward the uniquely defined ground state (where all  $\phi_i = 1$ ). Thus, there are no energy barriers in our idealized model system, and folding is therefore only limited by degeneracy/entropy barriers.

The zero temperature limit makes it possible to characterize the folding as function of number of subsequent folding steps, where one step is defined as an event where at least one term in the Hamiltonian becomes non-zero. Fig. 6a shows the time to fold subsequent steps of the Hamiltonian for a system of size  $N = 100$ . The (+) and (x) symbols denote trajectories of two different Hamiltonians of type (13), whereas the full line shows the ensemble averaged folding time (over all Hamiltonians and trajectories). We note that although the trajectories typically fold subsequent levels of the Hamiltonian, this is not necessarily the case, thus opening for alternate pathways.

Entropy barriers are caused by the necessity to fold several  $\phi_i$  terms simultaneously, and the chance to do this decreases as the  $1/2^k$ , where  $k$  is the number of terms. In Fig. 7a we display the entropy barrier  $dS/dk$  defined as the number of simultaneous folding terms versus the folding step  $k$  for the  $N = 100$  system. The histogram is  $dS/dk$  for one particular Hamiltonian, whereas the dashed line shows the barriers for the ensemble averaged values. Fig. 7b displays a data collapse of  $dS/dk$  for three different system sizes, demonstrating that both the position and the maximal barrier scale with system size approximately as  $\sqrt{N}$ , which implies that the folding time grows with systems size as  $2^{\sqrt{N}}$ . An argument for the obtained scaling is that after  $k$  folding steps, then as long as  $k$  is small, one typically has folded  $k^2/2$  terms. When  $k^2/2$  becomes comparable to  $N$ , overlap between subsequent steps becomes significant, and subsequent folding involves fewer new folding variables and therefore folding becomes easier.

In order to estimate whether these numbers are consistent with a fine grained behavior of real proteins then the degeneracy of each degree of freedom should be of the order of 6, corresponding to the orientational possibilities of a single amino acid on a random peptide chain. Thus exchanging  $2 \rightarrow 6$  in the above analysis, and noting that individual amino acids change conformations on a timescale of the order of nanoseconds [1], we very roughly estimate a folding time of  $6^{\sqrt{N}} \times 10^{-9}\text{s} \sim 10^{-1}\text{s}$  for  $N = 100$  which is of the order found for proteins.

Fig. 8a examines the zero temperature energy as function of folding step for a specific  $N = 40$  system, where we associate one unit of energy to each contact term in the Hamiltonian. Thus the coefficients  $a^{(i)} = 1$ , implying that all Hamiltonians of type (13) have equilibrium transition temperature  $T_c = 1/\log 2$ . The figure shows that the first  $k \sim 12$  steps is associated with a slow linear decrease in energy, hereafter a few subsequent steps is responsible for  $\sim 65\%$  of the total energy gain due to folding. Combining this with the fact that nearly all entropy reduction has to take place for  $k < 12$  (see Fig. 7), we conclude that entropy is reduced before energy is gained.

We now examine the effect of finite temperature where the increased importance of entropy converts entropy barriers into free energy barriers. This makes the initial folding steps thermodynamically disfavoured at temperatures below the equilibrium melting temperature  $T_c$ . In Fig. 8b this is examined quantitatively, where free energy is shown versus an effective order parameter  $u^*$ , defined as the number of  $\varphi$  variable which is equal to one and belongs to a term in the Hamiltonian which contributes a finite amount (i.e.  $E = 1$ ) to the energy. Thus  $u^*$  is linearly decreasing with the residual entropy of the system. The plot shows the free energy profile for three temperatures, the  $T = 0$  case, the temperature where folding becomes dynamically suppressed,  $T = T^* = 0.27T_c$  (for  $N = 40$ ), and the equilibrium denaturation temperature ( $T_c = 1/\log 2$ ) where the ground state just balances the denatured state. We conclude that in our simplified scenario, the sharpness of the transition at  $T_c$  arises because of an entropy barrier that will make folding much slower in some limited interval below the equilibrium melting temperature. With the parameters of the figure one first obtains the fairly fast folding examined in Fig. 6 when the temperature becomes below  $T^* \sim 0.27T_c$ .

We stress that one in principle could include energy barriers into our formalism by adding positive terms to the hamiltonian (i.e.  $-a_{ijk...}^{(n)} > 0$  in Eq. (13)). Such terms could arise either if the denatured state has binding contacts which are not in the native state or if the transition state have non native contacts. Here we focussed on the possibility for a transition that is purely limited by entropy barriers, thereby defining a transition state which has little entropy and large enthalpy difference to the ground state, a feature observed in for  $\alpha$ -spectrin SH3 by [27]. As a consequence we predict a temperature dependence that is opposite to recent measurement on protein folding kinetics, where typically the folding time decrease with temperature  $T$  for  $T < \sim 40^\circ\text{C}$  [27–29]. Energy barriers therefore plays a role at least at these lower temperatures. Future measurement of folding time behaviour close to the denaturation temperature could teach us whether the two-state behaviour found for folding of small proteins is due primarily to enthalpic or entropic barriers.

## V. CONCLUSION

In this paper we have explored the idea that entropy correlations and barriers may appear at any step during a sequential folding process. We have seen that this is natural to expect as consequence of a hierarchical folding

process where different branches of the hierarchical folding structure are correlated. We have showed that this folding scheme can result in two-state thermodynamics even though the energy gain is microscopically small at each folding step. We have seen that this two state thermodynamics can be merged with a fairly fast folding process, with time increasing with  $N$  as  $2^{\sqrt{N}}$  instead of  $2^N$  as one naively should expect for two-state folders. Further we have found the qualitatively same subdivision between initial and final folding as reported in [24], without the need to resorting to a special treatment of any terms. This subdivision into early entropically disfavoured guiding and last step easy match predicts a folding time that increases with temperature when denaturation is approached.

We thank A. Bakk and J. S. Høye for many fruitful discussions. P. G. D. thanks the NFR for financial support. P. G. D. and A. H. thank Nordita and the Niels Bohr Institute for friendly hospitality and support.

## APPENDIX A: CALCULATING THE AVERAGE PARTITION FUNCTION

We can make  $N!/m!$  different products of  $m$   $\phi_i$ . Thus, there is in total

$$M = \frac{N!}{(N-1)!} \frac{N!}{(N-2)!} \cdots \frac{N!}{(N-N)!} \quad (\text{A1})$$

different Hamiltonians (note, however, that most of them are equal up to permutations of  $\phi_i$ ).

We may calculate the mean value of the partition function

$$\begin{aligned} \langle Z \rangle &= \frac{1}{M} \sum_{\{a\}} \sum_{\{\phi\}} e^{-\mathcal{H}/T} \\ &= 1 + \frac{1}{M} \sum_{\{\phi\}} \sum_i e^{\phi_i/T} \sum_{i \neq j} e^{\phi_i \phi_j/T} \cdots \sum_{i \neq j \neq k \dots} e^{\phi_i \phi_j \phi_k \dots/T} \end{aligned} \quad (\text{A2})$$

The Hamiltonian is invariant to all permutations of  $\phi$ , and this suggests the new variable  $s = \sum_{i=1}^N \phi_i$ . We then find

$$\sum_i e^{\phi_i/T} = \frac{s!}{(s-1)!} e^{1/T} + \frac{N!}{(N-1)!} - \frac{s!}{(s-1)!}, \quad (\text{A3})$$

and

$$\sum_{i \neq j} e^{\phi_i \phi_j/T} = \frac{s!}{(s-2)!} e^{1/T} + \frac{N!}{(N-2)!} - \frac{s!}{(s-2)!}, \quad (\text{A4})$$

and so on. This gives us an expression for the mean partition function

$$\langle Z \rangle = 1 + \frac{1}{M} \sum_{s=1}^N \binom{N}{s} \prod_{k=1}^s \left[ \frac{s!}{(s-k)!} e^{1/T} + \frac{N!}{(N-k)!} - \frac{s!}{(s-k)!} \right] \prod_{k=s+1}^N \frac{N!}{(N-k)!}. \quad (\text{A5})$$

This expression can be further simplified to

$$\langle Z \rangle = 1 + \sum_{s=1}^N \binom{N}{s} \prod_{k=1}^s \left[ 1 + \frac{s!(N-k)!}{N!(s-k)!} (e^{1/T} - 1) \right]. \quad (\text{A6})$$

## APPENDIX B: FLUCTUATIONS OF PARTITION FUNCTION

In this Appendix, we find the expression for  $\langle Z^2 \rangle$  which was used to show that the relative fluctuations  $(\langle Z^2 \rangle - \langle Z \rangle^2)/\langle Z \rangle^2$  goes to zero as  $N \rightarrow \infty$ , as is seen in Fig. 3. We have that

$$\begin{aligned} \langle Z^2 \rangle &= \frac{1}{M} \sum_{\{a\}} \sum_{\{\phi\}} \sum_{\{\phi'\}} e^{-H(\phi)/T - H(\phi')/T} \\ &= \sum_{\{\phi\}} \sum_{\{\phi'\}} G(\phi, \phi'), \end{aligned} \quad (\text{B1})$$

where

$$G(\phi, \phi') = \sum_{\{\phi\}} \sum_{\{\phi'\}} \sum_i e^{(\phi_i + \phi'_i)/T} \sum_{i \neq j} e^{(\phi_i \phi_j + \phi'_i \phi'_j)/T} \dots \sum_{i \neq j \neq k \dots} e^{(\phi_i \phi_j \phi_k \dots + \phi'_i \phi'_j \phi'_k \dots)/T} . \quad (\text{B2})$$

The sum over  $\phi$  and  $\phi'$  is simplified by noting that the function  $G(\phi, \phi')$  is symmetric to all permutations of pairs  $(\phi_i, \phi'_i)$ . This means that  $G$  can be expressed as

$$G(\phi, \phi') = G(s, s', p) , \quad (\text{B3})$$

with  $s = \sum_{i=1}^N \phi_i$ ,  $s' = \sum_{i=1}^N \phi'_i$  and  $p = \sum_{i=1}^N \phi_i \phi'_i$ . The sum over all  $\phi_i$  and  $\phi'_i$  is thus reduced to a sum over  $s$ ,  $s'$  and  $p$ .

$$\begin{aligned} \langle Z^2 \rangle &= \frac{1}{M} \sum_{s=0}^N \sum_{p=p_{\min}}^s \binom{N}{p} \binom{N-p}{s-p} \binom{N-s}{s-p} G(s, s, p) \\ &\quad + \frac{1}{M} 2 \sum_{s=1}^N \sum_{s'=0}^{s-1} \sum_{p=p_{\min}}^{s'} \binom{N}{p} \binom{N-p}{s-p} \binom{N-s}{s'-p} G(s, s', p) , \end{aligned} \quad (\text{B4})$$

where  $p_{\min} = (s + s' - N)\Theta(s + s' - N)$ . The function  $G(s, s', p)$  is a product of  $N$  sums. Each sum can be evaluated. The results is

$$G(s, s', p) = \prod_{m=1}^N A_m(s, s', p) , \quad (\text{B5})$$

where we have that

$$\begin{aligned} A_m(s, s', p) &= \Theta(p - m) \frac{p!}{(p - m)!} e^{2/T} \\ &\quad + \left[ \Theta(s - m) \frac{s!}{(s - m)!} - \Theta(p - m) \frac{p!}{(p - m)!} \right] e^{1/T} \\ &\quad + \left[ \Theta(s' - m) \frac{s'!}{(s' - m)!} - \Theta(p - m) \frac{p!}{(p - m)!} \right] \\ &\quad e^{1/T} \\ &\quad + \frac{N!}{(N - m)!} + \Theta(p - m) \frac{p!}{(p - m)!} - \Theta(s - m) \frac{s!}{(s - m)!} - \Theta(s' - m) \frac{s'!}{(s' - m)!} . \end{aligned} \quad (\text{B6})$$

Here  $\Theta(n)$  is the step function ( $\Theta(n) = 1$  for  $n \geq 0$ ).

- 
- [1] T. E. Creighton, *Proteins: Structure and Molecular Properties*, 2nd ed. (Freeman, NY, 1993).
  - [2] S. T. Sun, I. Nishio, G. Swislow and T. Tanaka, The coil-globule transition: radius of gyration of polystyrene in cyclohexane, *J. Chem. Phys.* **73**, 5971-5975 (1980).
  - [3] P. L. Privalov, Intermediate States in Protein Folding *J. Mol. Biol.* **258**, 707-725 (1996).
  - [4] H. Frauenfelder, The Complexity of Proteins, in *Physics of Biological Systems*, ed. by H. Flyvbjerg, J. Hertz, M. H. Jensen, O. G. Mouritsen and K. Sneppen (Springer Verlag, Berlin, 1997).
  - [5] N.D. Socci, J. N. Onuchic, & P. G. Wolynes, Protein Folding Mechanisms and the Multidimensional Folding Funnel, *Proteins: Structure, Function and Genetics*, **32**, 136-158 (1998).
  - [6] K. A. Dill, S. Bromberg, K.-z. Yue, K. M. Fiebig, D. P. Yee, P. D. Thomas and H. S. Chan, Principles of Protein Science, *Protein Science*, **4**, 561-602 (1995).
  - [7] K. A. Dill, Polymer Principles and Protein Folding, *Protein Science*, **8**, 1166-1180 (1999).
  - [8] R. L. Baldwin and G. D. Rose, Is protein folding hierarchic? 1. Local structure and peptide folding, *TIBS*, **24**, 26-33 (1999).

- [9] R. L. Baldwin and G. D. Rose, Is protein folding hierarchic? 2. Folding intermediates and transition states, *TIBS*, **24**, 77-83 (1999).
- [10] A. R. Fersht, Protein folding and stability — the pathway of folding barnase, *FEBS Lett.* **325**, 5-16 (1993).
- [11] A. Hansen, M. H. Jensen, K. Sneppen and G. Zocchi, Statistical mechanics of warm and cold unfolding in proteins, *Europ. J. B*, **6**, 157-161 (1998).
- [12] A. Hansen, M. H. Jensen, K. Sneppen and G. Zocchi, A hierarchical scheme for cooperativity and folding in proteins, *Physica A*, **250**, 355-361 (1998).
- [13] A. Hansen, M. H. Jensen, K. Sneppen and G. Zocchi, Hot and cold denaturation of proteins: Critical aspects, *Europ. J. Phys. B*, **10**, 193-196 (1999).
- [14] K. A. Dill, K. M. Fiebig and H. S. Chan, Cooperativity in protein-folding kinetics, *Proc. Natl. Acad. Sci. USA*, **90**, 1942-1946 (1993).
- [15] P. -G. de Gennes, *Scaling Concepts in Polymer Physics* (Cornell University Press, Ithaca, 1993).
- [16] S. Miyazawa and R. L. Jernigan, Estimation of effective inter-residue contact energies from protein crystal structures: quasi-chemical approximation, *Macromolecules*, **18**, 534-552 (1985).
- [17] S. H. Huang, K. S. Ratliff, M. P. Schwartz, J. M. Spenner and A. Matouschek, Mitochondria unfold precursor protein by unraveling them from their N-termini, *Nature Struct. Biol.* **6**, 1132-1138 (1999).
- [18] S. Chakraborty and Z. -y. Peng, Hierarchical unfolding of the alpha-lactalbumin molten globule: Presence of a compact intermediate without a unique tertiary fold, *J. Mol. Biol.* **298**, 1-6 (2000).
- [19] D. T. Leeson, F. Gai, H. M. Rodriguez, L. M. Gregoret and R. B. Dyer, Protein folding and unfolding on a complex energy landscape, *Proc. Natl. Acad. Sci. USA*, **97**, 2527-2532 (2000).
- [20] Y. Wang and D. Shortle, The equilibrium folding pathway of staphylococcal nuclease: Identification of the most stable chain-chain interactions by NMR and CD spectroscopy, *Biochemistry*, **34** 15895-15905 (1995).
- [21] D. Shortle, Y. Wang, J. R. Gillespie and J. O. Wrabl, Protein folding for realists: A timeless phenomenon, *Protein Science*, **5** 991-1000 (1996).
- [22] P. L. Privalov and N. N. Khechinavili, A thermodynamic approach to the problem of stabilization of globular protein structure: A calorimetric study, *J. Mol. Biol.* **86**, 665-684 (1974).
- [23] P. L. Privalov, Thermodynamics of protein folding, *J. Chem. Thermodynamics*, **29**, 447-474 (1997).
- [24] A. Bakk, J. S. Høye, A. Hansen, K. Sneppen and M. H. Jensen, Pathways in two-state protein folding, submitted to *Biophys. J.* (2000).
- [25] B. Nolting, R. Golbik, J. L. Neira, A. S. Soler-Gonzales, G. Schreiber and A. R. Fersht, The folding pathways of a protein at high resolution from microseconds to seconds, *Proc. Natl. Acad. Sci. USA*, **94**, 826-830 (1997).
- [26] K. Binder, ed., *Applications of the Monte Carlo Method in Statistical Physics* (Springer Verlag, Berlin, 1987).
- [27] J. C. Martinez, A. R. Viguera, R. Berisio, M. Wilmanns, P. L. Mateo, V. V. Filimonov and L. Serrano, Thermodynamic Analysis of  $\alpha$ -spectrin SH3 and two of its Circular Permutants with Different Loop Lengths: Discerning the Reasons for Rapid Folding in Proteins, *Biochemistry* **38**, 549-559 (1999).
- [28] M. L. Scalley and D. Baker, Protein folding kinetics exhibit an Arrhenius temperature dependence when corrected for the temperature dependence of protein stability, *Proc. Natl. Acad. Sci. USA*, **94**, 10636-10640 (1997).
- [29] M. Oliveberg, Y. J. Tan, M. Silow and A. R. Fersht, The changing nature of the protein folding transition state: Implications for the shape of the free-energy profile for folding, *J. Mol. Biol.* **277**, 933-943 (1998).

FIG. 1. Folding pathways shown as a directed network between partially folded structures, which have been numbered.

FIG. 2. Folding pathway network corresponding to the hierarchical folding scheme described by Baldwin and Rose.

FIG. 3. Relative fluctuations of partition function for different temperatures as a function of system size  $N$ . This shows that the system is self averaging strongly enough, so that  $\log\langle Z \rangle = \langle \log Z \rangle$ .

FIG. 4. Order parameter  $u$  for  $N = 50, 100, 200$  as a function of temperature  $T$ .

FIG. 5.  $\alpha$  coefficient for different system sizes  $N$ .

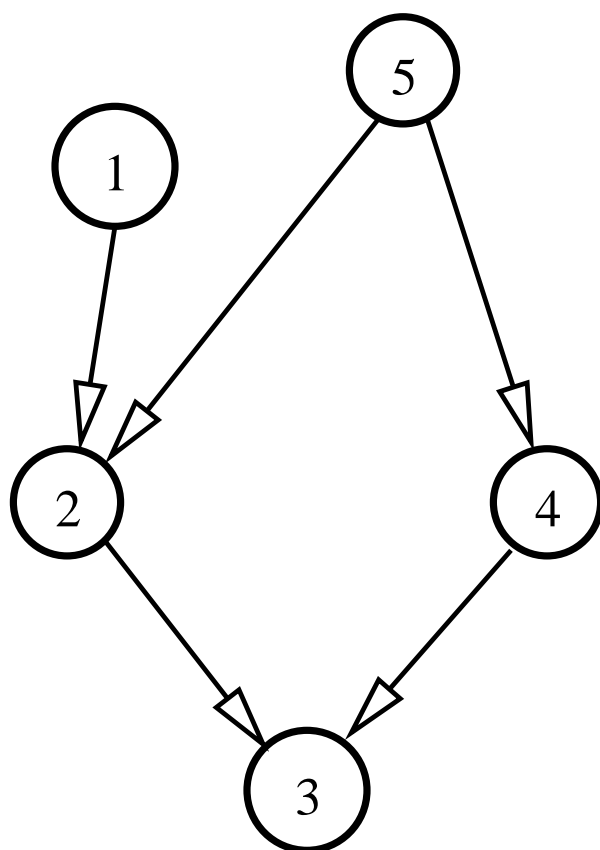
FIG. 6. a) Folding trajectories of  $N = 100$  systems. We show time since denatured state as function of folding step  $k$ . If all terms in Hamiltonian are assigned equal energy  $a = 1$ , each folding step is associated by one unit of energy reduction. The (+) symbols denote three trajectories for one Hamiltonian, the ( $\times$ ) symbols show three trajectories for another Hamiltonian. The full line shows the ensemble averaged folding trajectory. One observes that full folding is reached after about  $3 \cdot 10^5$  timesteps, and that it only require the first  $k \sim 20$  terms in the Hamiltonian to be explicitly folded.

FIG. 7. a) Folding barrier as function of folding step for the  $N = 100$  system. The largest folding barrier is caused by the maximum number of  $\phi$ -variables that must be set to one without guiding in order to make a term in the Hamiltonian non-zero. The (+) symbols illustrate a case where this barrier involves folding of 8  $\phi$  variables at folding step  $k = 9$ . b) Rescaled folding barriers  $((N/100)^{1/2} dS/dk)$  versus rescaled folding step  $((N/100)^{1/2} k)$  for three different system sizes ( $N = 25, 100$  and  $400$ ).

FIG. 8. a) Example of energy as function of folding step  $k$  for a system of  $N = 40$  folding variables and all terms in Hamiltonian assigned a prefactor  $a^{(i)} = 1$ . Note the distinct difference between early and late folding regime, contrasting the linear decrease found for the simple zipper model. b) Free energy versus effective order parameter (defined in Eq. (29)) for three different temperature. Note that the monotonic decrease at low temperature is replaced with a free-energy barrier at intermediate temperatures.

	$\phi_1$	$\phi_2$	$\phi_3$	$\phi_4$	$\phi_5$
1	1				5
2				4	4
3	2	2			2
4					
5	3	3	3	3	3

TABLE I. Folding table for the pathway network shown in Fig. 1. The columns refer to the variables  $\phi_i$ , while the rows refer to products of  $\phi_i$  variables. The left-most column refers to the number of  $\phi_i$ s in the products. The numbers to the right of the left-most column refer to the five structures in Fig. 1.



**Figure 1**

P.G. Dommersnes, A. Hansen, M.H. Jensen and K. Sneppen

*Parametrization...*

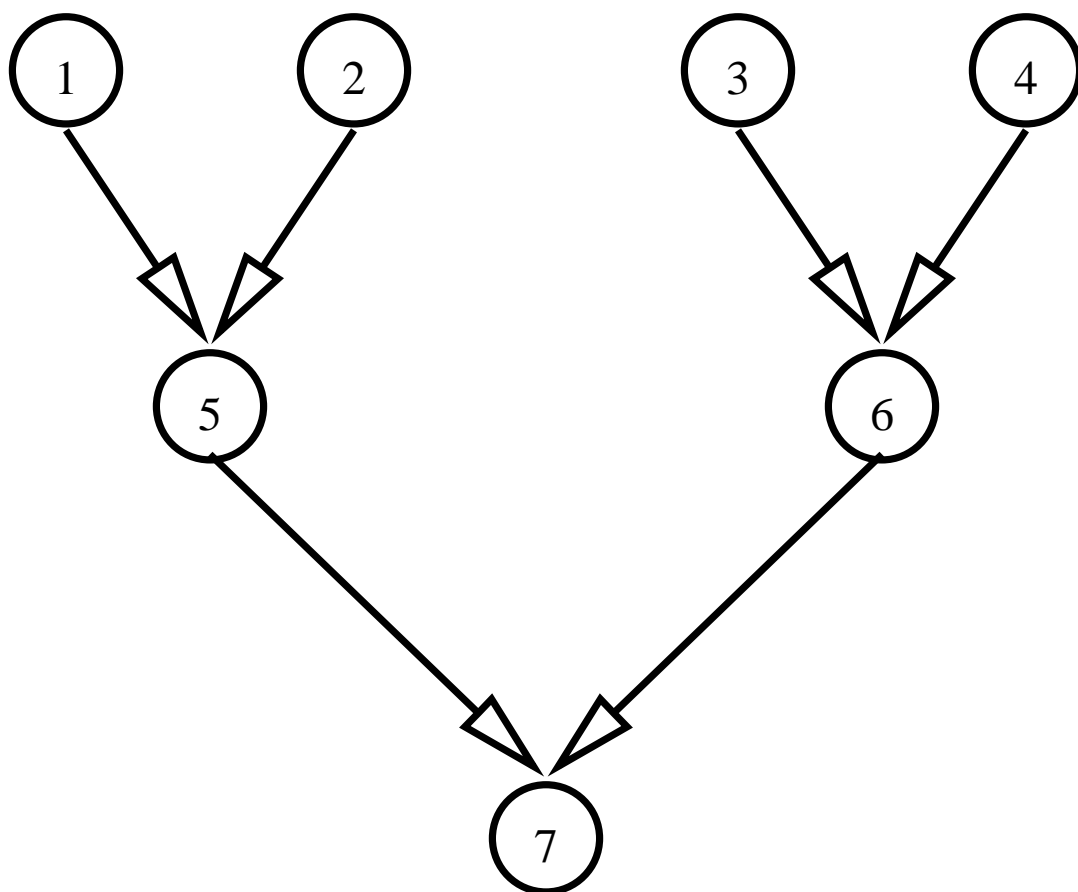


**Figure 2**

P.G. Dommersnes, A. Hansen, M.H. Jensen and K. Sneppen

*Parametrization...*

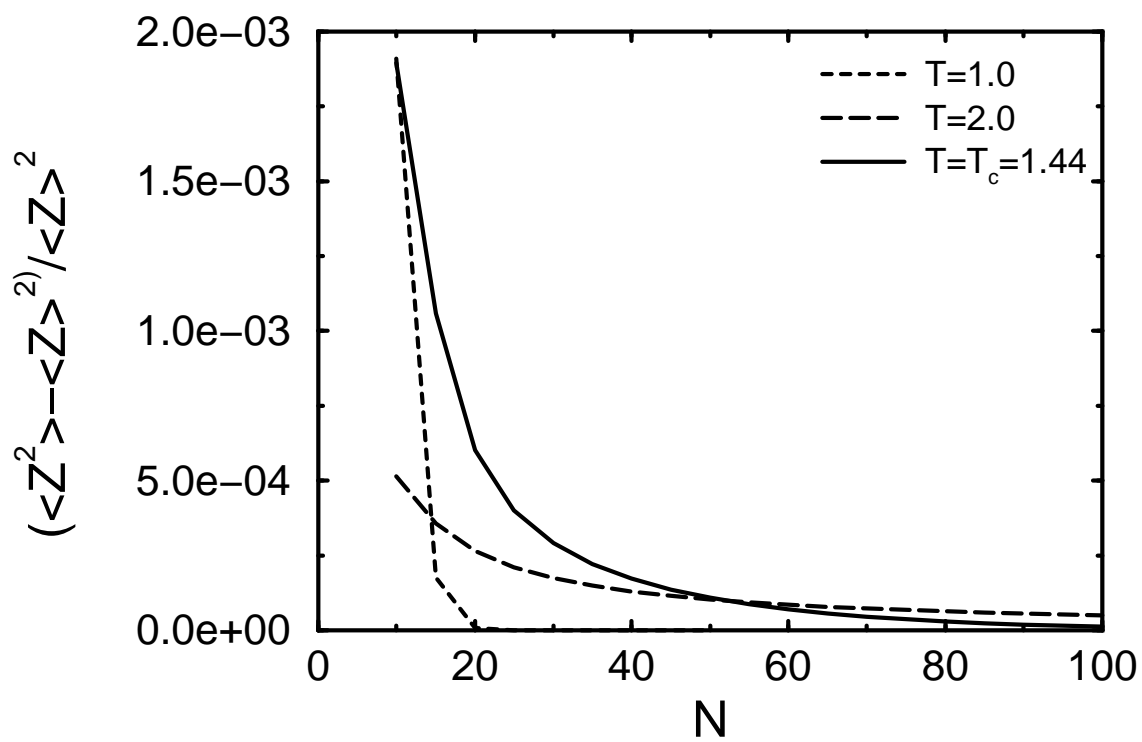


**Figure 3**

P.G. Dommersnes, A. Hansen, M.H. Jensen and K. Sneppen

*Parametrization...*



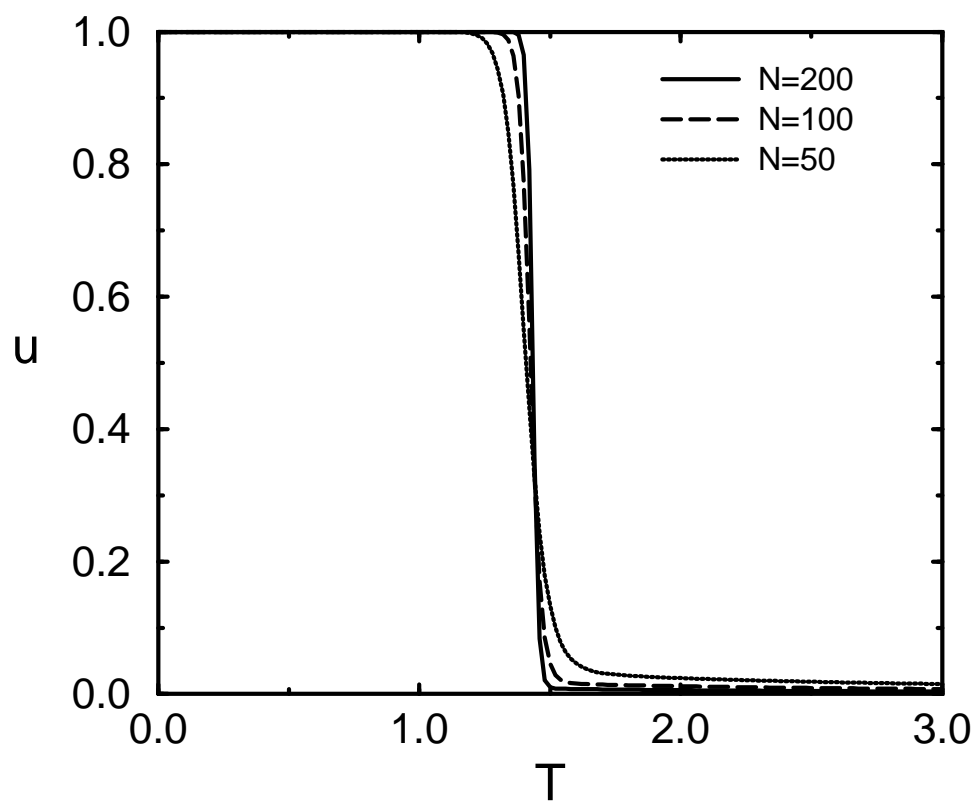


**Figure 4**

P.G. Dommersnes, A. Hansen, M.H. Jensen and K. Sneppen

*Parametrization...*

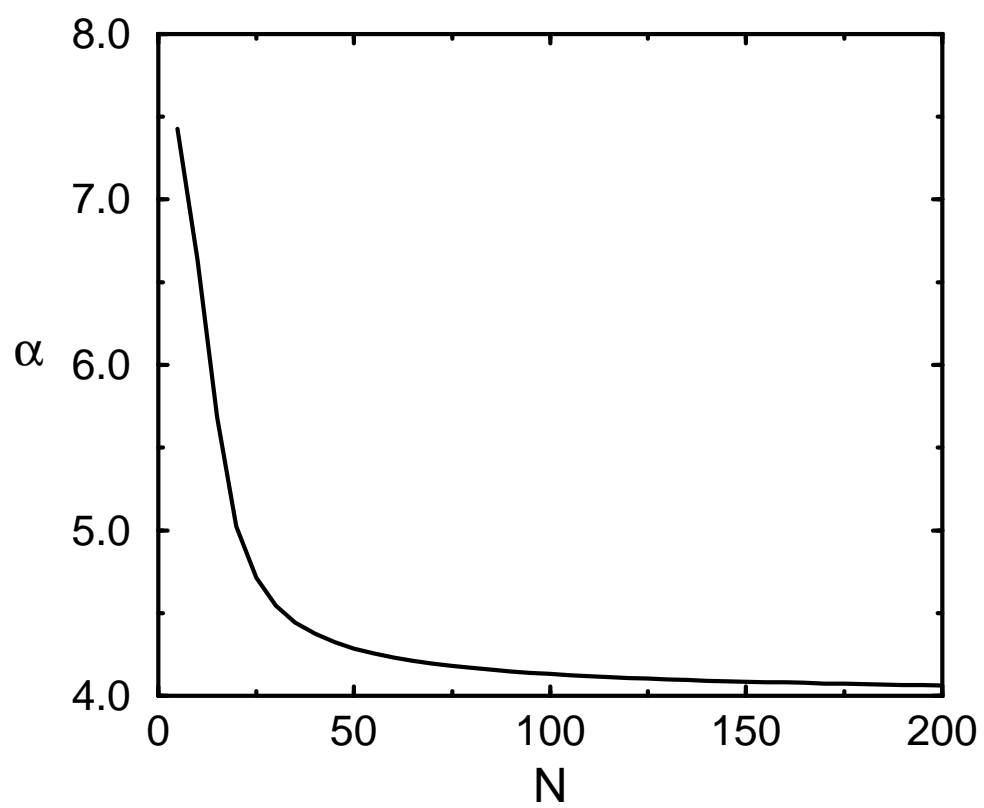


**Figure 5**

P.G. Dommersnes, A. Hansen, M.H. Jensen and K. Sneppen

*Parametrization...*

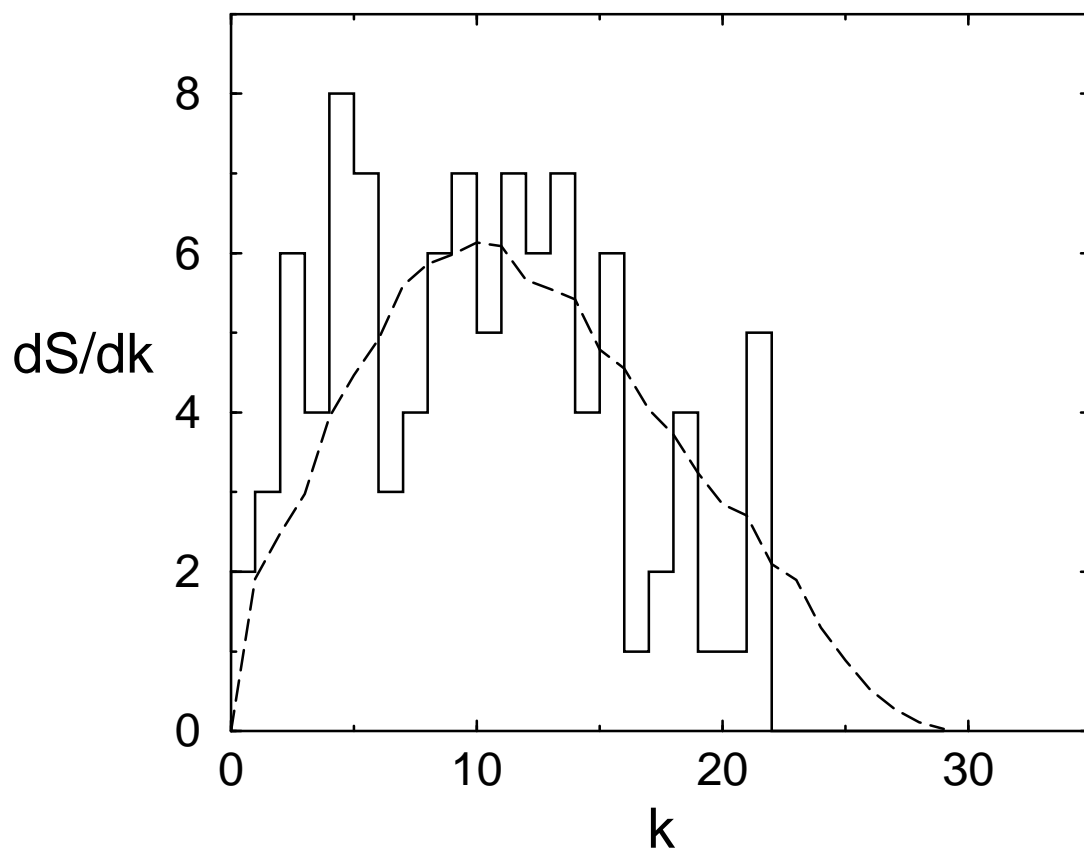


**Figure 6a**

P.G. Dommersnes, A. Hansen, M.H. Jensen and K. Sneppen

*Parametrization...*

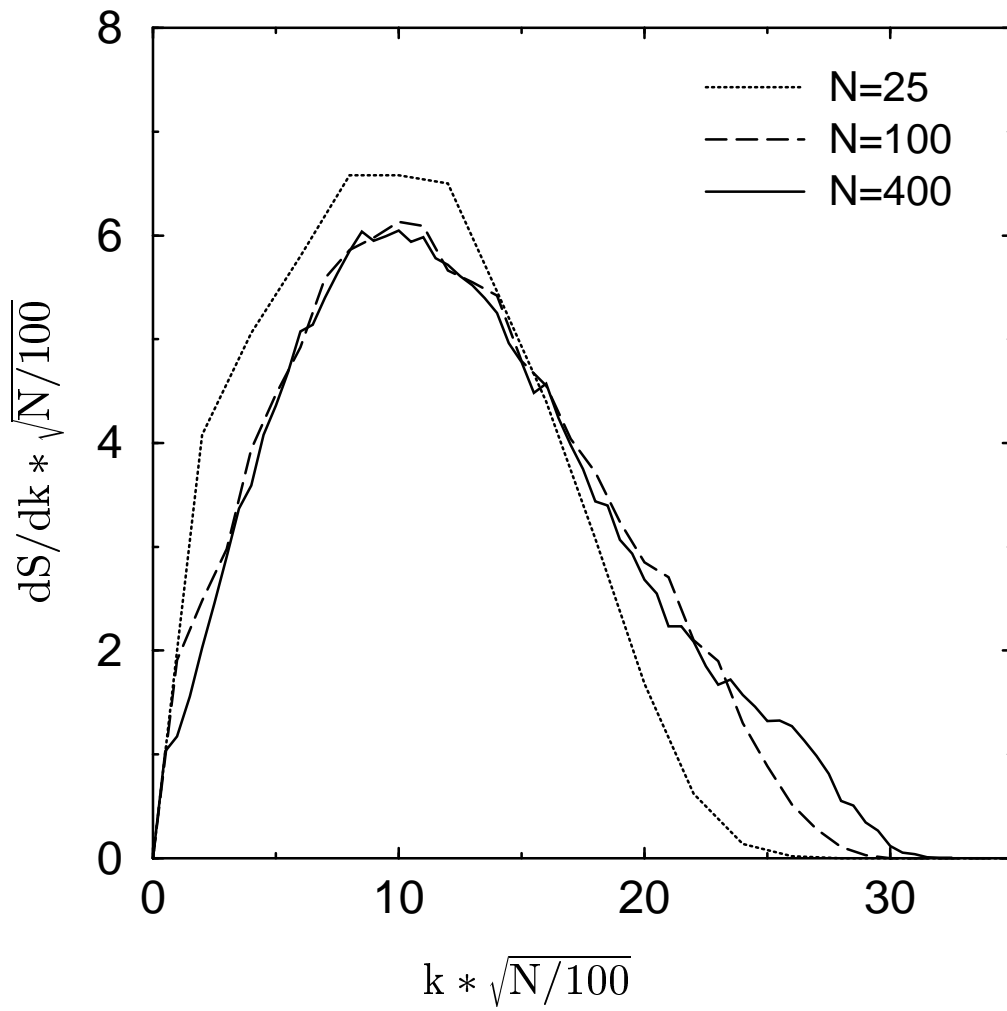


**Figure 6b**

P.G. Dommersnes, A. Hansen, M.H. Jensen and K. Sneppen

*Parametrization...*

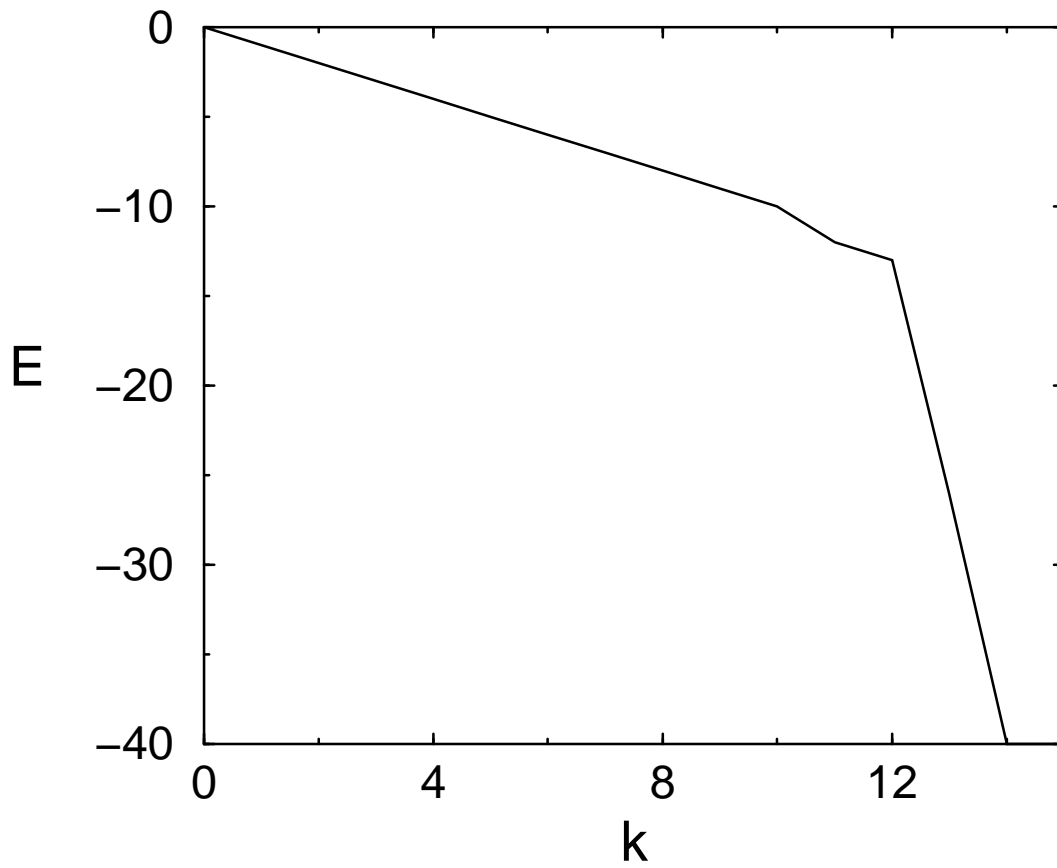


**Figure 7a**

P.G. Dommersnes, A. Hansen, M.H. Jensen and K. Sneppen

*Parametrization...*

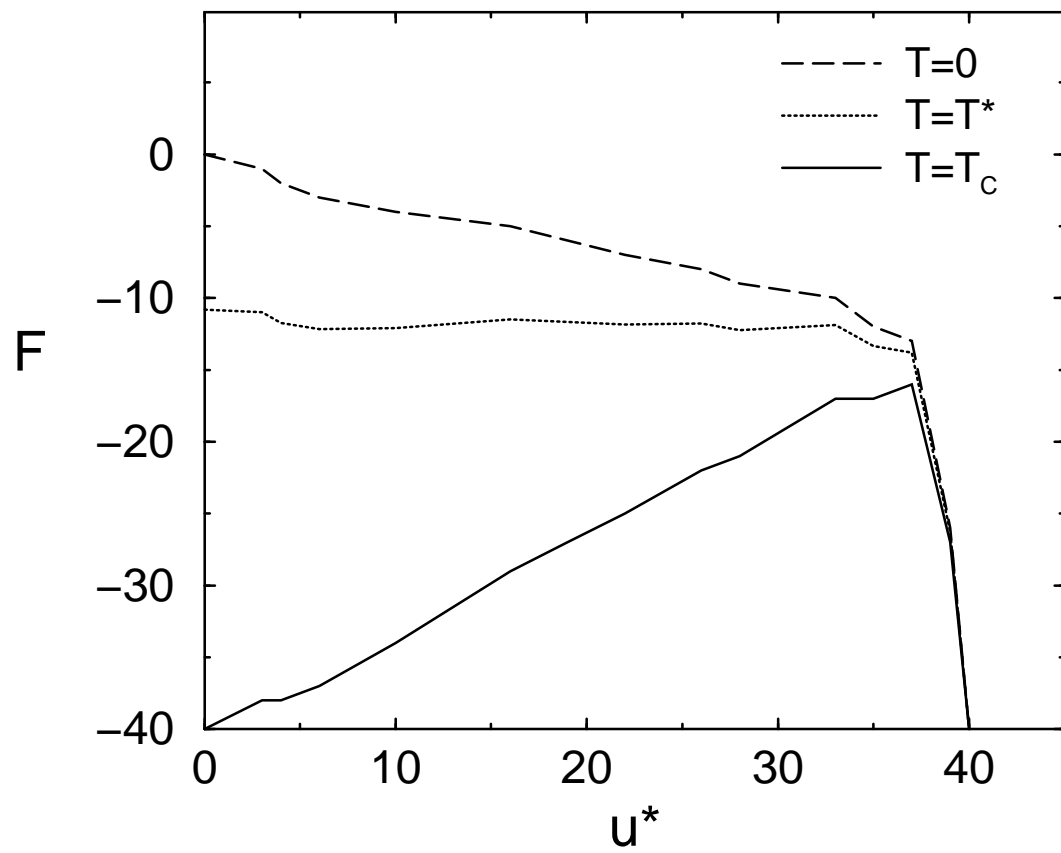


**Figure 7b**

P.G. Dommersnes, A. Hansen, M.H. Jensen and K. Sneppen

*Parametrization...*